THE THERMOPHYSICAL AND THERMOCHEMICAL PROPERTIES OF RuO$_2$ FROM 0 TO 1000 K

E. H. P. CORDFUNKE,† R. J. M. KONINGS,† E. F. WESTRUM, JR‡
and R. SHAVIV‡

†Netherlands Energy Research Foundation ECN, Petten, The Netherlands
‡Department of Chemistry, University of Michigan, Ann Arbor, MI 48109, U.S.A.

Abstract—The heat capacity from 5 to 350 K of RuO$_2$ has been measured by adiabatic calorimetry. For the thermochemical properties at room temperature C_p° (298.15 K) = (56.42 ± 0.08) J·mol^{-1}·K^{-1} and S° (298.15 K) = (46.15 ± 0.05) J·mol^{-1}·K^{-1} have been derived. Enthalpy increments relative to 298.15 K have been measured by drop calorimetry from 410 to 757 K:

$$\{H^\circ(T) - H^\circ(298.15\,\text{K})\}/\text{J} \cdot \text{mol}^{-1} = 53.6440(T/\text{K}) + 20.19049 \cdot 10^{-3}(T/\text{K})^2$$
$$+ 8.23298 \cdot 10^5(T/\text{K})^{-1} - 205501.1.$$

The thermodynamic functions, including the formation properties $\Delta_f H^\circ(T)$ and $\Delta_f G^\circ(T)$, have been derived for temperatures up to 1000 K.

Keywords: Ruthenium dioxide, calorimetry, thermophysics, thermodynamics, heat capacity, enthalpy increments, entropy.

1. INTRODUCTION

Ruthenium dioxide has remarkable physico-chemical properties. It has a high electrical conductivity being, like IrO$_2$ and OsO$_2$, a metallic conductor [1, 2]. Furthermore, it has interesting optical, magnetic and catalytic properties [3, 4].

Apart from this, ruthenium dioxide is of great interest in nuclear technology. The fission product ruthenium is a major constituent of the "white inclusions" in operating nuclear reactor fuel. The hexagonal white inclusions have been identified as a metallic solid solution of a number of transition metals, molybdenum being the other major component [5]. The formation of ruthenium dioxide in the UO$_2$ matrix will probably not normally occur since the oxygen potential in operating nuclear fuel is generally too low [6]. However, under accident conditions in water-cooled reactor fuel, the equilibrium conditions change drastically as a result of the interaction with the coolant, and formation of solid RuO$_2$ as well as the gaseous RuO$_3$ and RuO$_4$ molecules is possible. Accurate thermodynamic data for these compounds are needed to model the chemical processes occurring in nuclear accidents, especially the release as gaseous compounds to the containment building or, worse, the environment.

Up to now, a major problem in the evaluation of the Ru–O system was the lack of an accurate experimental determination of the standard entropy of RuO$_2$(s). Rard [7] derived S°(298.15 K) = (52.2 ± 8.7)J·mol^{-1}·K^{-1} from second-law analyses of EMF and decomposition measurements. Third-law analyses of vapour pressure measurements above RuO$_2$(s), to give the enthalpies of formation of

RuO$_3$(g) and RuO$_4$(g), as has been done by Rard, are consequently highly uncertain. Therefore, we decided to measure the low-temperature heat capacity of RuO$_2$ by adiabatic calorimetry, yielding an accurate value for the standard entropy. In addition, we performed drop calorimetric experiments covering the temperature range between the low-temperature data and previously reported high-temperature enthalpy increment measurements [8].

Using the results of the present study, we recently derived the standard enthalpy of formation of RuO$_2$(s) from EMF measurements [9]. With this value smoothed high-temperature thermodynamic functions have been calculated including the formation properties $\Delta_f H^\circ(T)$ and $\Delta_f G^\circ(T)$.

2. EXPERIMENTAL

The preparation of the RuO$_2$ sample via chlorination of ruthenium metal, has already been described [9]. The Ru-content was 75.84 ± 0.02% (calc. 75.96%).

Calorimetric techniques

The low-temperature heat capacity of RuO$_2$ was measured in an adiabatic calorimetric cryostat [10] (laboratory designated Mark XIII) over the temperature range 5–350 K (Table 1). A gold-plated, high conductivity, oxygen free, copper calorimeter (laboratory designation W-139) was used for both samples. The calorimeter has a mass of 13.21 g and an internal volume of 23 cm^3. The temperature of the calorimeter was measured with a Leeds & Northrup platinum encapsulated platinum resistance thermometer in an

Table 1. Molar heat capacities of RuO_2

T (K)	C_p° (J·mol⁻¹·K⁻¹)	T (K)	C_p° (J·mol⁻¹·K⁻¹)	T (K)	C_p° (J·mol⁻¹·K⁻¹)	T (K)	C_p° (J·mol⁻¹·K⁻¹)	T (K)	C_p° (J·mol⁻¹·K⁻¹)
Series I		25.53	0.652	55.08	5.016	135.55	25.453	216.85	43.593
6.09	0.049	26.95	0.758	58.19	5.688	141.09	26.840	222.99	44.696
6.93	0.043	28.39	0.876	61.31	6.398	146.65	28.213	229.15	45.782
7.82	0.059	29.92	1.016	64.74	7.193	152.21	29.590	235.30	46.879
8.68	0.067	31.55	1.179	68.45	8.060	157.77	30.955	241.46	47.920
9.54	0.083	33.18	1.362	72.19	8.948	163.36	32.267	248.14	49.024
10.38	0.099	34.92	1.569	76.24	9.958			255.33	50.118
11.30	0.119	36.75	1.804	80.59	11.095	Series III		262.52	51.215
12.31	0.137	38.76	2.080	84.95	12.263			269.70	52.281
13.35	0.153	40.96	2.407	89.58	13.486	155.91	30.506	276.87	53.823
14.38	0.170	43.17	2.755	94.47	14.854	161.77	31.887	284.09	54.521
15.43	0.190	45.57	3.168	96.95	15.370	167.86	33.302	291.28	55.598
16.56	0.218			99.39	15.856	173.95	34.707	298.46	56.480
17.76	0.251	Series II		104.34	17.250	180.05	36.120	305.66	57.290
18.95	0.293			109.29	18.515	186.16	37.505	312.84	58.019
20.17	0.343	44.63	2.975	114.27	19.848	192.29	38.829	320.02	58.661
21.39	0.402	46.98	3.420	119.26	21.169	198.43	40.111	327.20	59.402
22.71	0.473	49.58	3.906	124.51	22.576	204.57	41.315	334.40	60.133
24.11	0.558	52.20	4.422	130.03	24.048	210.71	42.471	341.11	60.770

entrant well. The thermometer was calibrated by the U.S. National Bureau of Standards against IPTS-48 [11] and is considered to reproduce the thermodynamic temperature scale within 0.03 K from 5–300 K.

About 17.6 g sample were put in the calorimeter. This represents about 0.132 moles when 133.07 g·mol⁻¹ is selected as the molecular mass. To facilitate rapid thermal equilibration 2.67 kPa at 300 K of helium gas were introduced into the calorimeter after evacuation. To avoid exposure to oxygen, the loading and the unloading of the calorimeter were performed in an oxygen-free atmosphere of a glove-box. At no time was the sample exposed to an atmosphere that contained more than 3 ppm of oxygen. The calorimeter containing the sample was sealed in the inert atmosphere and then reopened on the vacuum line for the introduction of helium. The calorimeter was then sealed, placed in the cryostat, and cooled. The heat capacity of the empty calorimeter represented 70–80% of the total heat capacity at temperatures below 50 K and became about 50–65% at higher temperatures.

The enthalpy increments above 298.15 K were measured in an isothermal diphenyl-ether calorimeter which has been described previously [12]. Briefly, the sample is enclosed in a spherical vitreous silica ampoule with a 0.6 mm wall thickness, a 20 mm diameter and a volume of 4.2 cm³. The ampoule is heated in a furnace whose temperature is measured with calibrated Pt (Pt + 10 mass per cent Rh) thermocouples to ±0.1 K. After a reasonable equilibration time, the ampoule is dropped into the calorimeter. The energy of the ampoule plus the sample now melts solid diphenyl-ether in equilibrium with its liquid in a closed system. The resulting volume increase of the ether is determined by weighing the displaced mercury. The ratio of heat input to mass of mercury making up the volume change is a constant for the

apparatus (79.977 ± 0.063)J·g⁻¹ and is obtained by calibration with α-SiO₂ and compared with the NBS standard reference material (No. 720), synthetic sapphire, Al_2O_3. Our results with sapphire all agree within 0.2% with the data given by the NBS. The enthalpy contributions of the vitreous silica were determined separately.

For the present measurements 6.80194 g of RuO_2 were enclosed in an ampoule of 1.39509 g; all masses being corrected for weighing in argon. The results of the 27 measurements are listed in Table 2. A

Table 2. Calorimetric enthalpy increment measurements of RuO_2

| T (K)	$\{H^\circ(T) - H^\circ(298.15\ K)\}$ (J·mol⁻¹) Exp.	Calc.	δ (%)
410.3	6862	6866	−0.06
429.6	8090	8138	−0.59
468.8	10776	10792	−0.15
489.0	12206	12193	0.11
507.7	13449	13511	−0.46
507.8	13416	13518	−0.75
508.1	13468	13539	−0.52
528.5	15033	14998	0.23
548.5	16510	16449	0.37
568.3	17884	17905	−0.12
573.0	18240	18254	−0.06
588.5	19492	19411	0.42
597.5	20187	20088	0.49
607.8	20818	20868	−0.24
627.7	22396	22389	0.03
637.5	23236	23145	0.39
648.2	23894	23975	−0.34
667.2	25484	25463	0.08
667.5	25496	25487	0.04
687.4	27049	27063	−0.05
688.3	27129	27135	−0.02
707.5	28644	28673	−0.10
716.9	29567	29433	0.46
727.9	30234	30326	−0.30
742.1	31513	31488	0.08
767.1	33511	33554	−0.13
757.3	32730	32741	−0.03
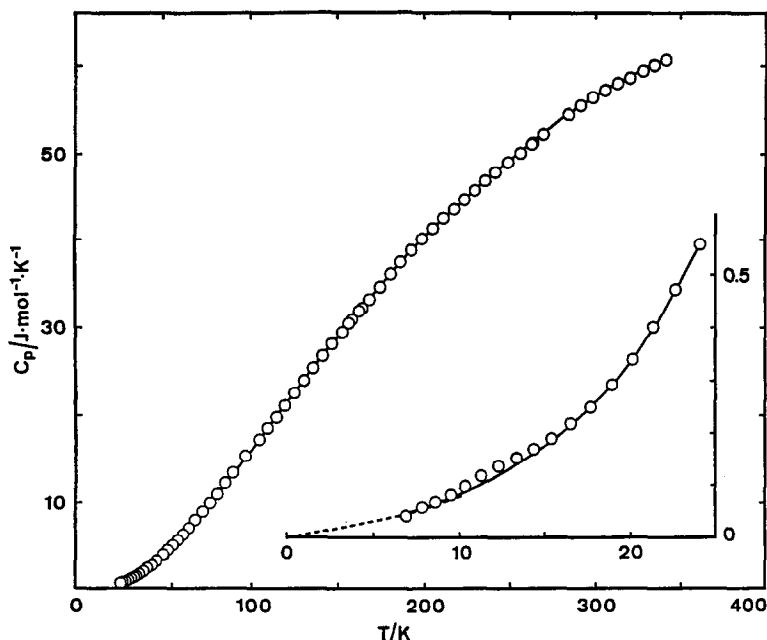
Fig. 1. The molar heat capacity of RuO$_2$. (O) This work; (---) Passenheim and McCollum [16].

correction was made for the difference in enthalpy between the final calorimeter temperature (300.06 K) and the standard reference temperature, 298.15 K, using C_p° (298.15 K).

3. RESULTS

The low-temperature heat capacity data are listed in Table 1 and plotted in Fig. 1. No special contributions other than that of the lattice and electronic contributions are observed in the entire temperature range of the experiment. Thermodynamic functions at selected temperatures are listed in Table 3. The thermodynamic functions were evaluated by extrapolating the experimental heat capacity curve to 0 K and by integrating. The computer program FITAB2 was used for all integrations and evaluations of thermodynamic functions [13], yielding at room temperature:

$$C_p^{\circ} (298.15 \text{ K}) = (56.42 \pm 0.08) \text{ J} \cdot \text{mol}^{-1} \cdot \text{K}^{-1}$$

and

$$S^{\circ} (298.15 \text{ K}) = (46.15 \pm 0.05) \text{ J} \cdot \text{mol}^{-1} \cdot \text{K}^{-1}.$$

The high-temperature enthalpy increments can be represented by the polynomial equation (410–757 K):

$$\{H^{\circ}(T) - H^{\circ}(298.15 \text{ K})\}/\text{J} \cdot \text{mol}^{-1}$$

$$= 53.6440(T/\text{K}) + 20.19049 \cdot 10^{-3}(T/\text{K})^2$$

$$+ 8.23298 \cdot 10^5 (T/\text{K})^{-1} - 20550.1.$$

As boundary conditions $\{H^{\circ}(T) - H^{\circ}(298.15 \text{ K})\} = 0$ at 298.15 K, and C_p° (298.15 K) = 56.42 J·mol^{-1}·K^{-1} were applied. The standard deviation is 61 J·mol^{-1} or 0.33%.

The smoothed thermodynamic quantities at selected temperatures of RuO$_2$(s) from 298.15 to 1000 K are listed in Table 4. The formation properties were calculated from $\Delta_f H^{\circ}$ (298.15 K) = $-(314.15 \pm 0.02)$ kJ·mol^{-1} as reported by Cordfunke and Konings [9]. Auxiliary data for the reference state of ruthenium were taken from Cordfunke and Konings [14] and of oxygen from Glushko et al. [15].

4. DISCUSSION

There is good agreement between the low- and high-temperature results presented here. This is demonstrated in Fig. 2 in a $\{H^{\circ}(T) - H^{\circ}(298.15 \text{ K})\}/(T - 298.15 \text{ K})$ vs T plot, where both data sets join smoothly at 298.15 K.

Two previous heat-capacity measurements on this compound overlap in the lower and upper temperature range of the present measurements. Passenheim and McCollum [16] measured the heat capacities of RuO$_2$ between 0.54 and 10 K. The agreement with their results is good (Fig. 1). Frederickson and Chasanov [8] measured the enthalpy increments of RuO$_2$ from 619 to 1175 K, which agree reasonably well with the present results in the overlapping temperature range (i.e. 1.08–0.50%). Nevertheless, the fit with these results is not smooth, since the slopes of both lines clearly differ (see Fig. 2). Extrapolation of

Table 3. Thermodynamic properties at selected temperatures for RuO_2

T (K)	$C_p^o(T)$ (J·mol^{-1}·K^{-1})	$\{S(T) - S^o(0)\}$ (J·mol^{-1}·K^{-1})	$\{H^o(T) - H(0)\}$ (J·mol^{-1})	$-\{G^o(T) - H^o(0)\}$K (J·mol^{-1}·K^{-1})
0	0	0	0	0
10	0.091	0.050	0.32	0.017
20	0.333	0.175	2.25	0.067
30	1.023	0.424	8.62	0.133
40	2.262	0.873	24.61	0.258
45	3.068	1.189	37.89	0.349
50	3.991	1.555	55.48	0.449
60	6.086	2.469	105.63	0.707
70	8.439	3.575	178.09	1.031
80	10.950	4.864	274.95	1.430
90	13.536	6.311	397.37	1.887
100	16.147	7.865	545.76	2.411
110	18.757	9.528	720.28	2.985
120	21.376	11.274	920.99	3.600
130	23.979	13.087	1147.80	4.257
140	26.548	14.958	1400.48	4.955
150	29.059	16.878	1678.59	5.687
160	31.487	18.832	1981.41	6.444
170	33.840	20.811	2308.08	7.234
180	36.101	22.806	2657.86	8.040
190	38.288	24.818	3029.85	8.871
200	40.375	26.839	3423.29	9.720
210	42.362	28.859	3837.10	10.584
220	44.224	30.871	4270.27	11.457
230	45.970	32.875	4720.91	12.347
240	47.633	34.871	5198.02	13.245
250	49.238	36.841	5673.74	14.151
260	50.834	38.803	6174.27	15.057
270	52.414	40.757	6690.59	15.972
280	53.952	42.686	7221.89	16.895
290	55.382	44.607	7768.97	17.818
298.15	56.422	46.153	8224.60	18.574
300	56.646	46.502	8329.36	18.741
310	57.735	48.381	8901.40	19.672
320	58.708	50.227	9483.40	20.595
330	59.672	52.048	10075.4	21.518
340	60.662	53.844	10677.4	22.441
350	61.593	55.623	11288.5	23.363

Table 4. Thermodynamic functions of RuO_2

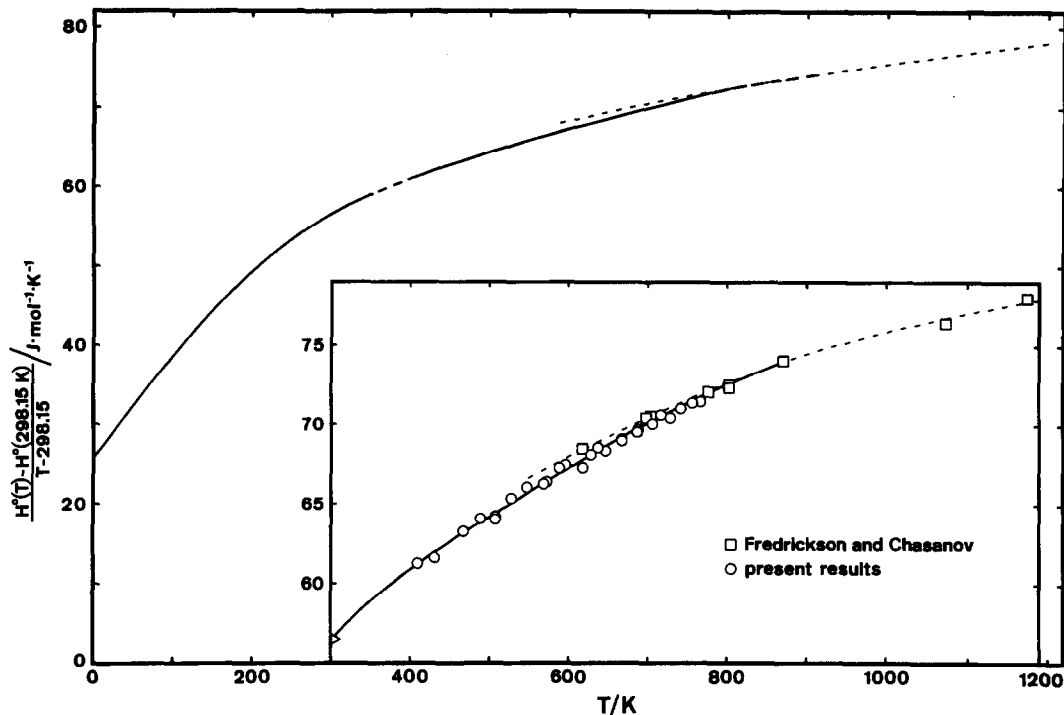| T (K)	$C_p^o(T)$ (J·mol^{-1}·K^{-1})	$S^o(T)$ (J·mol^{-1}·K^{-1})	$-[G^o(T) - H^o(298.15)]/T$ (J·mol^{-1}·K^{-1})	$(H^o(T) - H^o(298.15\ K))$ (J·mol^{-1})	$\Delta_f H^o(T)$ (J·mol^{-1})	$\Delta G_f^o(T)$ (J·mol^{-1})
298.15	56.422	46.150	46.150	0	−314,200	−258,298
300	56.611	46.500	46.151	105	−314,194	−257,952
400	64.651	63.969	48.478	6196	−313,524	−239,287
500	70.541	79.051	53.119	12,966	−312,349	−220,855
600	75.586	92.367	58.572	20,277	−310,820	−202,695
700	80.230	104.371	64.270	28,070	−308,989	−184,814
800	84.662	115.375	69.890	36,316	−306,873	−167,216
900	88.970	125.597	75.598	44,999	−304,475	−149,901
1000	93.202	135.190	81.082	54,108	−301,793	−132,865

Fig. 2. The reduced enthalpy increment functions: (——) smoothed fit from the low-temperature and high-temperature enthalpy measurements; (O) experimental points; and (— — —) smoothed fit from the results of Fredrickson and Chasanov [8].

the Fredrickson and Chasanov data to lower temperatures will thus give values which deviate strongly from the present results.

To examine the experimental results in greater detail the low-temperature heat-capacity data were fitted by the recently developed Komada/Westrum model for determination of lattice heat capacity [17, 18]. This model is computer-aided and requires several physical parameters. The parameters can be related either to the molar volume of the compound, or to the mass relationships between the elements in the compound. Other parameters involve the chemical formula, and the number of such units in a primitive cell. Based upon the input parameters the model calculates an approximation to the phonon density of states, which in turn is used to calculate an apparent characteristic temperature θ_{kw} for the compound. The calculation of this characteristic

temperature is based only on the lattice heat capacity. The separation of the lattice and the electronic heat capacities was done by fitting the data for temperatures below 13 K to a third-order polynomial

$$C_p = \gamma T + \alpha T^3.$$

A plot of C_p/T vs T^2 reveals that a straight line can be drawn to fit the data. The coefficients gamma and alpha are found to be $3.611 \cdot 10^{-3}$ J·mol^{-1}·K^{-2} and $5.46.10^{-5}$ J·mol^{-1}·K^{-4}, respectively. When the apparent characteristic temperature for RuO$_2$ is plotted as a function of temperature (Fig. 3) it can be seen that θ_{kw} is a constant for temperatures larger than 15 K. This result illustrates that no additional contributions to the lattice contribution are observed in the current study.
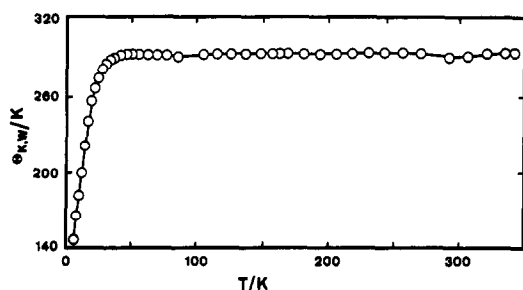

Fig. 3. The Komada–Westrum characteristic temperature θ_{kw} of RuO$_2$ as a function of temperature.

REFERENCES

1. Butler S. R. and Gillson J. L., *Mater. Res. Bull.* **6**, 81 (1971).
2. Pizzini S., Buzzanca G., Mari C., Rossi L. and Torchio S., *Mater. Res. Bull.* **7**, 449 (1972).
3. Huang Y. S., Park H. L. and Pollak F. H., *Mater. Res. Bull.* **17**, 1305 (1982).
4. Kleyn M., Thesis, University of Wageningen, The Netherlands (1987).
5. Kleykamp H., Paschoal J. O., Pejsa R. and Thümmler F., *J. nucl. Mater.* **130**, 426 (1985).
6. Cordfunke E. H. P. and Konings R. J. M., *J. nucl. Mater.* **152**, 301 (1988).

7. Rard J. A., *Chem. Rev.* **85**, 1 (1985).
8. Fredrickson D. R. and Chasanov M. G., *J. chem. engng Data* **17**, 21 (1972).
9. Cordfunke E. H. P. and Konings R. J. M., *Thermochim. Acta* **129**, 63 (1988).
10. Westrum E. F., Jr, Furukawa G. T. and McCullough J. P., in *Experimental Thermodynamics* (Edited by J. P. McCullough and D. W. Scott), Vol. I, p. 133. Butterworths (1968); Komada N., Westrum E. F., Jr, *J. chem. Thermodynamics* (scapolite) (submitted).
11. Stimson H. F., *J. Res. natl Bur. Stand.* **65A**, 139 (1961).
12. Cordfunke E. H. P., Muis R. P. and Prins G., *J. chem. Thermodynamics* **11**, 819 (1979).
13. Justice B. H., Thermal data fitting with orthogonal functions and combined table generation. The FITAB Program Project Report COO-1149-143, February 1969. Department of Chemistry, The University of Michigan, An Arbor.
14. Cordfunke E. H. P. and Konings R. J. M., *Thermochim. Acta* **139**, 99 (1989).
15. Glushko V. P., Gurvich L. V., Bergman G. A., Veits I. V., Medvedev V. A., Khachkuruzov G. A. and Yungman V. S., *Termodinamicheskie svoistva individualnykh veskchestv.* Nauk, Moskva (1978).
16. Passenheim B. C. and McCollum D. C., *J. chem. Phys.* **51**, 320 (1969).
17. Westrum E. F., Jr and Komada N., *Thermochim. Acta* **109**, 11 (1986).
18. Komada N. and Westrum E. F., Jr, *J. chem. Thermodynamics* (submitted).